Hydrol. Earth Syst. Sci. Discuss., https://doi.org/10.5194/hess-2017-415
Manuscript under review for journal Hydrol. Earth Syst. Sci.
Discussion started: 19 July 2017

Hydrology and Earth System Sciences
Open Access
EGU
Discussions

Evaporation suppression and energy balance of water reservoirs covered with self-assembling floating elements

Milad Aminzadeh, Peter Lehmann, Dani Or

Department of Environmental Systems Science, ETH Zurich, Switzerland

Correspondence to: Milad Aminzadeh (milad.aminzadeh@usys.ethz.ch)

Abstract. The growing pressure on natural fresh water resources and projected climate variability would expand the need for water storage during rainy periods. Evaporative losses present a challenge to efficient water storage reservoirs, especially in arid regions with chronic water shortages. Among the various methods for suppressing evaporative losses, the use of self-assembling floating elements offers a simple and scalable solution especially for small reservoirs. The use of floating elements is not new, yet the science behind the design and the resulting performance including other effects on the water body remain empirical. We propose a systematic approach for modeling the energy balance and fluxes from covered water surfaces considering element geometry, radiative properties and local conditions. The water energy balance equation was linked to the energy balance of floating discs on the surface of reservoir to consider the effect of surface coverage and cover properties on radiative energy storage within the water body and surface heat fluxes. The modeling results demonstrated significant drop in evaporative losses from covered reservoirs where incoming radiative flux is primarily intercepted by the cover surface and released into the atmosphere in form of long wave radiation and sensible heat fluxes

Hydrol. Earth Syst. Sci. Discuss., https://doi.org/10.5194/hess-2017-415
Manuscript under review for journal Hydrol. Earth Syst. Sci.
Discussion started: 19 July 2017

yielding much higher Bowen ratio over covered relative to uncovered water reservoirs. The theoretical approach provides a scientific basis for an important water resource protection strategy and a predictive framework for design purposes.

1 Introduction

The competition over dwindling fresh water resources is expected to intensify with projected increase in human population and expansion of irrigated land (Assouline et al., 2015), and with changes in precipitation and drought patterns (Dai et al., 2011). Present global storage capacity for reservoirs > 0.1 km^3 is about 6200 km^3, with estimated total storage volume of 8070 km^3 when smaller reservoirs are considered resulting in total evaporating surface area exceeding 300000 km^2 (Lehner et al., 2011). The reliance on water storage in reservoirs (Figure 1) is likely to increase to mitigate seasonal shortages due to projected precipitation variability, and to meet water needs for increased population and food production. By some estimates up to half of stored water in small reservoirs is lost to evaporation (Craig, 2005; Rost et al., 2008) thereby exacerbating the water scarcity problem. Interest in methods for suppressing evaporation have led to upsurge in the use of self-assembling floating covers over water reservoirs (e.g., Los Angeles reservoir in Sylmar, California), yet the selection, performance and implementation of such measures remain largely empirical. Recent studies (Assouline et al., 2011; Ruskowitz et al., 2014) have shown that evaporation suppression is a highly nonlinear process that depends on the properties of the covers (size, radiative properties and shape).

This study aims to provide a scientific basis for using self-assembling floating covers to suppress evaporative losses from reservoirs. The available strategies include deepening the water reservoirs (to

reduce evaporative surface per stored volume), covering the surface, underground storage, or introducing wind breakers to reduce exchange with wind. Among these different measures for evaporation suppression, the use of self-assembling floating elements appears most promising for small-scale reservoirs due to its simplicity, cost-effectiveness and scalability (Craig, 2005; Assouline et al., 2011; Gallego-Elvira et al., 2012; Chaudhari and Chaudhari, 2015). Floating covers spontaneously rearrange in response to changes in water level or external conditions, e.g., wind (in contrast with chemical films that may break up due to the wave action, UV radiation, or biological activity).

Laboratory studies of evaporation from partially covered water surfaces (Assouline et al., 2010; Assouline et al., 2011) suggest nonlinear relationship between the covered area fraction and evaporative losses (see Figure 1 in Assouline et al. (2011)). These nonlinearities are attributed to vapor diffusion from water gaps across air viscous boundary layer (Schlünder, 1988; Shahraeeni et al., 2012; Haghighi et al., 2013) and potential feedback on the gap temperature (Aminzadeh and Or, 2013). The combined effects of gap size, spacing and thickness of the air boundary layer (Shahraeeni et al., 2012) support laboratory experimental results of Assouline et al. (2011) that have shown higher evaporation rates from small water gaps (per unit gap area) relative to evaporation rates from larger gaps (with similar uncovered surface fraction). These nonlinear relationships and additional energetic constraints must be considered in design and deployment of evaporation suppression floating covers.

In contrast with mass transfer from partially covered water surfaces, the quantification of energy partitioning over these surfaces remains largely empirical with limited predictive capabilities beyond calibrated scenarios (Yao et al., 2010; Gallego-Elvira et al., 2011). The incoming radiative energy is

intercepted primarily by the floating covers that may increase the cover temperature depending on its geometry, radiative properties (albedo and emissivity), and heat conduction and capacity of the floating element material. The absorbed heat flux may be transferred to the water body in contact with floating covers, or return to the atmosphere as emitted long wave radiation and sensible heat flux. Interactions of floating elements with air flow regimes over the surface (turbulent or laminar) may generate complex aerodynamic patterns that affect sensible heat flux from surface elements.

The thermal coupling between floating cover elements and the water body has seldom been considered systematically by investigating surface energy balances for water and covers (Cooley, 1970). A few studies have considered this aspect via changes in heat storage of the water body as deduced from measurements (Gallego-Elvira et al., 2012). As the covered area fraction increases, the increase in intercepted radiative energy over the floating elements and their potential warming up may increase (lateral) heat fluxes towards water gaps thereby contributing to enhanced vapor flux from the uncovered water surface fraction (Aminzadeh and Or, 2017). Additionally, the decrease in the radiative energy penetrating into the water body affects the heat storage and aspects of biological activity within the reservoir. Hence, consideration of the energy balance over water surfaces covered by floating elements is a critical ingredient for any design and management of evaporation suppression from water reservoirs.

The objectives of this study are to: (1) mechanistically model energy storage and surface fluxes of uncovered and partially covered water reservoirs; (2) consider the effect of cover properties on surface

Hydrol. Earth Syst. Sci. Discuss., https://doi.org/10.5194/hess-2017-415
Manuscript under review for journal Hydrol. Earth Syst. Sci.
Discussion started: 19 July 2017

heat fluxes and radiative energy storage in a reservoir; and (3) predict evaporation suppression efficiency of floating covers.

In the following, the theoretical considerations of energy balance for uncovered and partially covered reservoirs are presented. We then investigate evaporation suppression efficiency of floating discs and their effects on surface heat fluxes and radiative energy storage in a small reservoir.

2 Modeling framework

2.1 Energy balance and evaporation from uncovered water reservoirs

Before considering evaporation suppression from covered reservoirs, we first quantify fluxes from the uncovered reservoir as the reference state. The quantification of the temperature profile within the water body is the key to defining surface heat fluxes and thus radiative energy storage into the reservoir. For simplicity, we employed a one-dimensional energy balance equation with subsurface radiation absorption and diffusive heat transfer including molecular and eddy thermal diffusivity to describe the vertical temperature profile in a reservoir according to (Dake and Harleman, 1969; Vercauteren et al., 2011):

$$\frac{\partial T_w}{\partial t} = \frac{\partial}{\partial z}\left(\left(\alpha_{T,w} + D_w\right)\frac{\partial T_w}{\partial z}\right) + \frac{Q(z,t)}{\rho_w c_w} \quad (1)$$

where T_w is water temperature at depth z, $\alpha_{T,w}$ is molecular thermal diffusion, D_w is eddy thermal diffusivity, ρ_w and c_w are density and specific heat of water, respectively, and Q is the heat source due

Hydrol. Earth Syst. Sci. Discuss., https://doi.org/10.5194/hess-2017-415
Manuscript under review for journal Hydrol. Earth Syst. Sci.
Discussion started: 19 July 2017

to the absorption of radiative flux within the water body that is a function of depth (light attenuation) and time (diurnal/seasonal variation of incoming radiation) (Dake and Harleman, 1969):

$$Q(z,t) = \eta(1-\beta)(1-\alpha_w)R_s(t)\,\mathrm{e}^{-\eta z} \tag{2}$$

where β is the absorption coefficient of incoming solar radiation (R_s) at the water surface, α_w is water surface albedo and η is the light attenuation coefficient. Alternatively, the heat source term can be quantified based on the dependence of light attenuation on wavelength (Rabl and Nielsen, 1975; Vercauteren et al., 2011). Among different formulations for quantification of eddy thermal diffusivity that governs heat transfer within the water body (McCormick and Scavia, 1981; Malacic, 1991; Vlasov and Kelley, 2014), we opt the analytical representation based on Henderson-Seller (1985) which describes D_w as a function of depth, density and friction velocity at the surface (that is a function of wind speed over the reservoir):

$$D_w = \frac{ku_s^* z}{P_0}\exp(-k^* z)[1+37R_i^2]^{-1} \tag{3}$$

where k is von Karman's constant, P_0 is the neutral value of turbulent Prandtl number, u_s^* is the friction velocity at the water surface that is characterized based on friction velocity of the air flow at the surface (u_a^*):

$$u_s^* = \sqrt{\frac{\rho_a}{\rho_w}}u_a^* \tag{4}$$

The parameter k^* is a function of latitude (ϕ) and wind speed (U):

Hydrol. Earth Syst. Sci. Discuss., https://doi.org/10.5194/hess-2017-415
Manuscript under review for journal Hydrol. Earth Syst. Sci.
Discussion started: 19 July 2017

$$k^* = 6.6\sqrt{\sin\phi}\,U^{-1.84} \tag{5}$$

and R_i is the Richardson number:

$$R_i = \frac{-1+\left(1+40N^2k^2z^2/(u_s^{*2}\exp(-2k^*z))\right)^{1/2}}{20} \tag{6a}$$

in which:

$$N^2 = \frac{-g}{\rho_w}\left(\frac{\partial\rho_w}{\partial z}\right) \tag{6b}$$

The bottom boundary condition in deep reservoirs is often considered at constant temperature or zero heat flux. In shallow reservoirs, one must consider the energy balance at the reservoir bottom and heat exchange with soil profile beneath. Hence, in a shallow reservoir with depth *D*, the energy balance at the bottom and related heat flux are expressed as:

$$\rho_w c_w(\alpha_{T,w}+D_w)\left.\frac{\partial T_w}{\partial z}\right|_{z=D} = (1-\beta)(1-\alpha_w)R_{s,D}(t)+\frac{k_s}{Z}(T_{sZ}-T_D) \tag{7}$$

where k_s is the effective thermal conductivity of the soil layer beneath the reservoir, $R_{s,D}$ is the shortwave radiation intercepted at the bottom of reservoir, T_D is the bottom temperature of the reservoir (assumed similar to the water temperature at $z=D$), and T_{sZ} is a linearized soil temperature at thermal decay depth Z (Shahraeeni and Or, 2011; Aminzadeh and Or, 2014). The water surface energy exchange expressed in terms of radiative, sensible and latent heat fluxes governs the surface boundary condition for Eq. (1):

Hydrol. Earth Syst. Sci. Discuss., https://doi.org/10.5194/hess-2017-415
Manuscript under review for journal Hydrol. Earth Syst. Sci.
Discussion started: 19 July 2017

Hydrology and Earth System Sciences
Discussions

$$\rho_w c_w \alpha_{T,w} \left.\frac{\partial T_w}{\partial z}\right|_{z=0} = \beta(1-\alpha_w)R_s(t) + \sigma(\varepsilon_a T_a^4 - \varepsilon_w T_{ws}^4) + h_a(T_a - T_{ws}) - \frac{D_a L}{\delta}(C_s(T_{ws}) - C_a) \quad (8)$$

where α_w is water surface albedo, σ is the Stefan-Boltzmann constant, ε_a and ε_w are atmospheric and water surface emissivity, respectively, T_{ws} is water surface temperature, T_a is the air temperature, h_a is the sensible heat flux coefficient, D_a is the vapor diffusion coefficient in air, L is the latent heat of vaporization, δ is the thickness of air boundary layer that is a function of wind speed (Haghighi and Or, 2013), C_s is saturated vapor concentration at the water surface and C_a is the vapor concentration in air mass. The sensible heat flux coefficient is quantified as (Gaikovich, 2000; Aminzadeh and Or, 2014; Haghighi and Or, 2015a):

$$h_a = \frac{k_a}{\delta} \quad (9)$$

in which k_a is the air thermal conductivity.

Often, an unstable temperature profile develops in the water column where a cold water layer may form above a warmer layer due to subsurface radiation absorption; such conditions trigger convective mixing in natural reservoirs. Typically, mixing processes in the water body may require complex (higher dimensional) modeling of flows; however, for simplicity, we opted for a simple 1D mixing approach of Dake and Harleman (1969) that results in a uniform temperature within a mixed layer of water while conserving energy (see Figure 2):

$$\int_0^{h_m} (T_w - T_m)\, dz = 0 \quad (10)$$

Hydrol. Earth Syst. Sci. Discuss., https://doi.org/10.5194/hess-2017-415
Manuscript under review for journal Hydrol. Earth Syst. Sci.
Discussion started: 19 July 2017

where T_m and h_m are temperature and vertical thickness of the surface mixed layer, respectively. Solution of Eq. (1) results in vertical temperature profile and thus surface heat fluxes including evaporative loss from the reservoir.

The inflows and outflows of water in a reservoir may alter the heat storage of the water body, especially in multiuse reservoirs (e.g., releases for electrical energy production in dams). The net advected heat into the reservoir is characterized by the volume-weighted heat content of water inflows and outflows (Moreo and Swancar, 2013):

$$Q_V = \sum_i \rho_w c_w V_i (T_i - \overline{T}) - \sum_e \rho_w c_w V_e (T_e - \overline{T}) \quad (11)$$

where Q_V is the rate of change in heat content due to the changes in water budget of the reservoir; V_i and T_i, and V_e and T_e are the rates and mean temperatures of inflows and outflows, respectively, and $\overline{T}$ is the mean temperature of the reservoir. The parameter Q_V can be considered in terms of a heat source/sink (e.g., similar to the radiation absorption) to investigate the effect of heat advection due to water exchanges on the energy balance and thus temperature profile in a reservoir.

2.2 The energy balance of partially covered reservoirs

The use of floating cover elements aimed to suppress evaporative losses also modifies interactions of the reservoir surface with overlying air flow and thus wind-driven subsurface mixing patterns. The interception of radiative flux by the cover surface decreases radiation penetration into the water body shifting the energy partitioning to the cover surface. To simplify the analyses, we consider the energy

Hydrol. Earth Syst. Sci. Discuss., https://doi.org/10.5194/hess-2017-415
Manuscript under review for journal Hydrol. Earth Syst. Sci.
Discussion started: 19 July 2017

balance of a reservoir covered by floating Styrofoam discs (similar to the laboratory experiments in Appendix A). A covered reservoir surface (Figure 3a and b) is represented by a unit cell comprised of a floating disc surrounded by water gaps whereby the ratio of cover area to the total unit cell area defines the surface coverage (Figure 3c). We thus modify the surface boundary condition of the reservoir while retaining a simple 1D formulation and considering energy exchanges with the airflow and floating elements:

$$\rho_w c_w \alpha_{T,w} \left.\frac{\partial T_w}{\partial z}\right|_{z=0} = f_w \left(\beta(1-\alpha_w) R_s(t) + \sigma(\varepsilon_a T_a^4 - \varepsilon_w T_{ws}^4) + h_a(T_a - T_{ws}) - \varphi \frac{D_a L}{\delta_e}(C_s(T_{ws}) - C_a) \right) + f_c \, q_c \qquad (12)$$

where f_w and f_c are the areal fractions of free and covered surface, respectively ($f_w = 1 - f_c$), and δ_e represents an effective air boundary layer thickness over the partially covered reservoir. The parameter φ accounts for the aerodynamic enhancement of vapor flux from relatively small water gaps in comparison with the thickness of viscous sublayer (Assouline et al., 2011). Hence, the reduction of vapor diffusion resistance from individual gaps due to the formation of three-dimensional vapor shells (governed by the combined effect of gap size a_g, boundary layer thickness and lateral spacing) would enhance vapor diffusion and result in values of $\varphi \geq 1$ (Schlünder, 1988; Shahraeeni et al., 2012):

$$\varphi = \frac{1}{f_w + \frac{a_g}{\delta_e}\sqrt{\frac{f_w}{\pi}}\left(\sqrt{\frac{\pi}{4 f_w}} - 1\right)} \qquad (13)$$

This expression becomes effective for gap sizes much smaller than the boundary layer thickness.

Hydrol. Earth Syst. Sci. Discuss., https://doi.org/10.5194/hess-2017-415
Manuscript under review for journal Hydrol. Earth Syst. Sci.
Discussion started: 19 July 2017

Due to the strong lateral mixing induced by air flow at the reservoir surface (relative to the scale of water gaps), we assume a uniform horizontal temperature at the water surface that is defined based on the heat exchanges with air and conductive flux between floating elements and water surface (q_c) via Eq. (12). Hence, the energy balance equation of the floating disc in the unit cell is used to quantify temperature distribution of the cover and thus the conductive heat exchange with water:

$$\frac{1}{\alpha_{T,c}}\frac{\partial T_c}{\partial t}=\frac{1}{r}\frac{\partial}{\partial r}(r\frac{\partial T_c}{\partial r})+\frac{\partial^2 T_c}{\partial h^2} \quad (14)$$

in which T_c is cover temperature at radial coordinate r and thickness h, and $\alpha_{T,c}$ is molecular thermal diffusivity of cover material. The boundary condition at the surface and periphery of disc in contact with air flow is governed with radiative and sensible heat fluxes while we assume that the bottom of the disc in contact with water surface has the same temperature as water. Simultaneous solution of Eqs. (1) and (14) enables quantification of temperature profiles in water body and floating elements that are linked via conductive heat flux (q_c).

The air flow friction velocity (u_a^*) and the effective thickness of viscous sublayer over the partially covered reservoir (δ_e) are determined using the analyses of Haghighi and Or (2015b) for evaporating porous surfaces covered with bluff body obstacles obtained based on the theory of drag partitioning over rough surfaces (Shao and Yang, 2008; Nepf, 2012) (see appendix B for details).

Hydrol. Earth Syst. Sci. Discuss., https://doi.org/10.5194/hess-2017-415
Manuscript under review for journal Hydrol. Earth Syst. Sci.
Discussion started: 19 July 2017

3 Results and discussions

3.1 Model evaluation for uncovered water reservoirs

The energy balance equations were solved numerically using the finite difference method (forward time-central space scheme). Modeling results of vertical temperature profile and surface heat fluxes for the uncovered water reservoir were evaluated using data from Lake Mead, USA (Moreo and Swancar, 2013). We have used hourly meteorological data (air temperature and humidity, wind speed, and solar radiation) measured at Lake Mead (March 2010 to February 2011) to estimate the evolution of vertical temperature profile. Figure 4 compares our model estimations of mean monthly temperature profiles with water temperature measured at different depths (Moreo and Swancar, 2013). The assumed thermal and radiative properties of the lake (and covers) are listed in Table 1. The measured and simulated fluxes are summarized in Table 2 showing good agreement between modeled and measured annual net radiation (R_n) and evaporation (LE) fluxes. The model overestimates the reported sensible heat flux (H) that was estimated by Moreo and Swancar (2013) based on the Bowen ratio method with associated energy closure issues (Foken, 2008; Kalma et al., 2008).

These results for temperature profile and energy fluxes of uncovered water reservoir provide a reference state for investigating effects of partial coverage on heat storage and energy balance of reservoirs.

3.2 The energy budget of partially covered water reservoirs

Covering a water reservoir with floating elements affects absorption of radiative energy at the surface and consequently the water body heat storage and temperature profile. We were unable to obtain reservoir scale data for model validation (e.g., data from the Los Angeles reservoir is not publically

Hydrol. Earth Syst. Sci. Discuss., https://doi.org/10.5194/hess-2017-415
Manuscript under review for journal Hydrol. Earth Syst. Sci.
Discussion started: 19 July 2017

available); we thus opted for a synthetic case using FLUXNET data from Majadas (Spain) as a dry region with significant atmospheric evaporative demand for the water year from March 1, 2004 to March 1, 2005. The potential effects of floating elements on heat fluxes and water temperature profiles within a hypothetical reservoir were evaluated using half-hourly meteorological data.

Figure 5 shows model predictions for the evolution of mean daily temperature profile of uncovered and covered reservoir using white and black Styrofoam discs in a (hypothetical) reservoir with depth of 10 m. As expected, the highest water temperature of uncovered reservoir occurs during summer with a warm layer of water at top of the reservoir whose temperature decreases monotonically to the bottom while convective thermal mixing and low radiative flux yield an almost uniform vertical temperature profile at the end of winter and beginning of spring. The reservoir was then assumed to be covered by Styrofoam discs with diameter of 0.2 m and thickness of 0.02 m providing a surface overage of 0.91 (maximum packing of discs). Due to the geometry of floating elements and their density on the surface (cover areal fraction), the effective thickness of air boundary layer was calculated similar to the thickness of boundary layer over uncovered water reservoir (Appendix B). This result obtained based on the theory of drag partitioning over surfaces covered with bluff body obstacles was independently supported with isothermal modeling of evaporation from a water surface covered with similar discs using COMSOL Multiphysics.

The mean daily temperature profiles of the reservoir covered with white and black discs depicted in Figures 5 clearly demonstrate that covering the surface with floating elements yields a much colder reservoir. Surprisingly, despite large difference in surface albedo of black and white discs (see Table 1),

the resulting water temperature profile did not vary much between these two types of floating covers. We attribute this to the strong insulating properties of the Styrofoam that energetically decouples the top of cover with different temperature and flux conversions from the water surface. Considering the low thermal diffusivity of Styrofoam discs that yields negligible heat conduction to the water body, the intercepted radiative flux on the cover surface results in the increase of cover temperature (Figure 6a). Although the radiative properties of the floating cover may slightly affect the water surface temperature (Figure 6b) and the evaporative flux from covered reservoir (Figure 7c), the cover surface temperature and thus sensible and radiative heat fluxes change drastically.

In the following section, we investigate the effect of surface coverage and cover properties on the evolution of surface heat fluxes.

3.2.1 Surface fluxes from partially covered reservoirs

The evolution of surface heat fluxes over the uncovered and partially covered reservoir is shown in Figure 7. The reflection of incoming shortwave radiation by the cover surface resulted in a decrease in net radiative flux of the covered reservoir. The impact of surface albedo on net radiative flux is evident with changing the cover color yielding lower net radiation over the reservoir covered with white discs relative to the reservoir that is covered with black discs.

The effect of floating discs on evaporation from the reservoir illustrated in Figure 7c indicates that discs significantly suppress evaporative flux relative to uncovered water reservoir especially during summer. The substantial decrease in evaporative flux from covered reservoir with concurrent increase in sensible heat flux (due to the high cover temperature) results in a higher Bowen ratio over the covered reservoir

Hydrol. Earth Syst. Sci. Discuss., https://doi.org/10.5194/hess-2017-415
Manuscript under review for journal Hydrol. Earth Syst. Sci.
Discussion started: 19 July 2017

relative to water surfaces (Priestley and Taylor, 1972). Interestingly, the color of the floating discs did not affect evaporation suppression from the covered reservoir (also observed in the laboratory experiments in Appendix A); hence, the higher sensible heat flux from the black discs yields higher Bowen ratio relative to the white discs scenario. A summary of mean annual surface heat fluxes for uncovered and covered reservoir is presented in Table 3.

The ratio of heat storage into the water body relative to the net radiation over the surface of the uncovered and partially covered reservoir is shown in Figure 8. While this ratio for the uncovered water reservoir has a maximum value during summer following annual variation of radiative flux, it remains almost constant during the year for the partially covered reservoir with slight increases during summer. Moreover, the lower net radiative flux of the reservoir covered with white discs (Figure 7) results in higher values of the ratio of heat storage to the net radiation while subsurface heat storage does not change significantly with changing color of floating discs.

We have also investigated the effect of reservoir depth on energy storage and surface heat fluxes and a summary of results is provided in Appendix C.

3.2.2 Evaporation suppression efficiency of floating elements

Self-assembling floating discs effectively cover the reservoir and decrease water surface exposure to the atmosphere. We plotted the ratios of evaporative fluxes from covered water reservoirs relative to uncovered water surface (E_c / E) to quantify evaporation suppression efficiency of the floating discs (i.e., $\varepsilon = 1 - E_c / E$). The results in Figure 9 demonstrate that application of discs yields more than 80%

Hydrol. Earth Syst. Sci. Discuss., https://doi.org/10.5194/hess-2017-415
Manuscript under review for journal Hydrol. Earth Syst. Sci.
Discussion started: 19 July 2017

drop in evaporative loss from the reservoir ($E_c / E < 0.2$) with highest efficiency during summer. This result was obtained based on the 1D modeling of vapor flux ($\varphi = 1$) from relatively big water gaps between neighboring discs (diameter of 0.2 m) representing the upper bound of evaporation suppression efficiency. However, under certain conditions where the boundary layer thickness (often in the order of a few millimeters (Haghighi and Or, 2013)) is comparable with gap size (a_g / δ_e in Eq. 13), aerodynamic enhancement of vapor flux from individual gaps may decrease the suppression efficiency.

The evaporation ratio larger than the uncovered areal fraction (0.09) is attributed to the higher water surface temperature in gaps between floating elements relative to the uncovered water surface as illustrated in Figure 6b. The high evaporative loss from uncovered water reservoir results in more surface temperature depression and thus lower saturated vapor concentration relative to the vapor concentration at the surface of water gaps over partially covered reservoirs. The higher gap temperature relative to the uncovered water obtained from the modeling was also observed in laboratory experiments (Figure A2) supporting the nonlinearity of evaporation suppression from partially covered reservoirs.

Although we assumed air temperature and humidity obtained from FLUXNET measurements are the same over uncovered and partially covered reservoir, note that the higher sensible heat flux over covered reservoir could locally increase air temperature in contact with water gaps that, in turn, enhances evaporative loss from covered reservoir and decreases evaporation suppression efficiency.

Hydrol. Earth Syst. Sci. Discuss., https://doi.org/10.5194/hess-2017-415
Manuscript under review for journal Hydrol. Earth Syst. Sci.
Discussion started: 19 July 2017

3.3 Ecological considerations

Reservoirs may serve multiple functions including the support of various ecosystems, hence, the introduction of opaque floating covers to supress evaporation may alter water temperature, light penetration and gas exchange all affecting the ecology and life in the reservoir. The full consideration of ecological targets is beyond the scope of this study, clearly, certain parameters could be included in the cover design and management to limit adverse impacts on the ecology of the water body (in some cases, a cover may supress toxic algal blooms in a reservoir). For example, here we consider effects of floating covers on gas exchange across the air-water interface as a function of uncovered fraction (f_w). The oxygen transfer at the surface of reservoir (F_{s,O_2}) is expressed as (Stefan et al., 1995; Schladow et al., 2002):

$$F_{s,O_2} = f_w \, k_{s,O_2} (C_{e,O_2} - C_{w,O_2}) \tag{15}$$

where k_{s,O_2} is the oxygen transfer coefficient, and C_{e,O_2} and C_{w,O_2} are equilibrium oxygen concentration and oxygen concentration in the surface layer, respectively. The dissolved oxygen in the water body is consumed by aerobic organisms (e.g., fish and aquatic microorganisms) and affects various chemical reactions in a reservoir (Stefan et al., 1995). The mechanical sheltering impact of surface covers that dampens wind-driven mixing at the surface may affect air-water oxygen exchange and transport in water column yielding a stratified oxygen profile in the reservoir. Although the interception of radiative flux by the cover surface decreases subsurface radiation absorption and results in a colder reservoir that may enhance oxygen solubility in water (Wilkinson et al., 2015), the reduction of radiation absorption

Hydrol. Earth Syst. Sci. Discuss., https://doi.org/10.5194/hess-2017-415
Manuscript under review for journal Hydrol. Earth Syst. Sci.
Discussion started: 19 July 2017

limits convective mixing driven by unstable temperature profiles and intensifies a stratified oxygen distribution. Moreover, the photosynthesis by aquatic plants and microorganisms in darker and colder reservoirs covered with floating elements decreases which then affects the oxygen budget according to the oxygen transfer equation (Stefan et al., 1995):

$$\frac{\partial C}{\partial t} = \frac{\partial}{\partial z}\left(\left(\alpha_{O_2} + D_w\right)\frac{\partial C}{\partial z}\right) + P_{O_2} - R_{O_2} \quad (16)$$

where C is oxygen concentration at time t and depth z, α_{O_2} is molecular oxygen diffusion, and P_{O_2} and R_{O_2} are oxygen production by photosynthesis and consumption due to biological activities within the water body, respectively. In summary, exchange rates and oxygen production and concentration in a reservoir are strongly dependent on water temperature, radiative flux, transport processes and nutrients that are likely to be influenced by surface coverage. Such ecological objectives become part of the reservoir cover design where evaporation suppression must be balanced by ecological constraints.

3.4 Costs and water savings

The significant reduction in evaporative loss from the reservoir could be gauged by direct economic impact in terms of cost of alternate source of water where available. The economic efficiency of evaporation suppression depends on the costs of construction and annual maintenance of covers (i.e., P_c [\$/m^2] and P_m [\$/m^{2}year], respectively), alternate water cost (w [\$/m^3]), annual evaporation from the uncovered reservoir surface (E [m/year]), and evaporation suppression efficiency of floating covers (ε

Hydrol. Earth Syst. Sci. Discuss., https://doi.org/10.5194/hess-2017-415
Manuscript under review for journal Hydrol. Earth Syst. Sci.
Discussion started: 19 July 2017

) (Cooley, 1983; Assouline et al., 2011). Assuming a life span of Y years for the floating elements, the economic efficiency per unit area of reservoir (ζ [\$/m^2]) is estimated as:

$$\zeta = Y(\varepsilon w E - P_m) - P_c \quad (17)$$

We thus calculate ζ for the hypothetical reservoir presented in section 3.2 with annual evaporative losses for uncovered surface E=1.6 m/year, and estimated cover efficiency ε=0.8. Considering water price w=1 \$/m^3 (e.g., seawater reverse osmosis costs are in the range of 0.5 to 3 \$/m^3 (Gilau and Small, 2008; Guler et al., 2015)) floating cover cost P_c=5 \$/m^2 (based on commercially available HDPE floating balls) and cover maintenance cost P_m=0.1 \$/m^{2}year, the economic efficiency of such floating elements for a period of 5 years is ~1 \$/m^2. Hence, for a reservoir with 100×100 m^2 surface area, water costs saving equivalent to \$10000 is feasible in 5 years operation (along with 64000 m^3 of water protected from evaporation).

Tacit in this standard estimate is availability of an alternate water source (e.g., desalinated water); whereas in many regions in the world with poor infrastructure and acute water shortages, the value of evaporation suppression may transcend such estimates and the real measure could be expressed in terms of livestock supported by the additional water or avoidance of crop failure.

4 Summary and conclusions

Evaporative loss from local water storages in dry regions accounts for up to 50% of the stored water used to guarantee municipal, industrial and agricultural water supply in dry seasons (Shilo et al., 2015). Self-assembling floating elements offer an efficient and cost-effective measure for suppressing

evaporative loss from water reservoirs. Despite the wide application of floating elements, modeling evaporation and energy balance of covered reservoirs is often addressed empirically or limited to simple scenarios where salient features of cover properties and energy exchange between reservoir and floating elements are ignored.

We employed the water energy balance equation with an implicit convective mixing approach to quantify surface fluxes and vertical temperature profile in a water reservoir. Model estimations of temperature profile and evaporative flux were in good agreement with measurements at Lake Mead (USA) (Moreo and Swancar, 2013) providing a framework for considering energy balance of partially covered water reservoirs using floating elements. Simultaneous solution of energy balance equations in water body and floating elements linked via heat exchanges between cover and water surface enabled quantifications of surface heat fluxes and energy storage within the water body. Modeling results for a hypothetical reservoir covered with white and black Styrofoam discs demonstrated that interception of radiative flux by floating covers significantly decreases subsurface radiative energy absorption in covered reservoirs yielding colder water storages relative to uncovered water reservoirs. The intercepted radiative flux on the surface of floating elements that primarily increases cover temperature is released in form of sensible heat flux and long wave radiation into the atmosphere depending on the cover thermal and radiative properties.

Our modeling results showed more than 80% reduction in evaporative loss from a reservoir covered with Styrofoam discs. Reduction of evaporative loss along with higher sensible heat flux over partially

covered reservoir results in much higher Bowen ratio relative to uncovered water surfaces (Priestley and Taylor, 1972).

Floating elements efficiently suppress evaporative loss from water reservoirs and alter energy storage within the reservoir and oxygen exchange at the water-air interface. Notwithstanding theoretical considerations of evaporation and energy balance of covered reservoirs in the present study which primarily aimed to provide a physically based framework for design purposes, certain ecological aspects including light and oxygen transmission associated with multiuse reservoirs need to be addressed systematically. Clearly, detailed field scale experimental studies of evaporation from partially covered reservoirs are required to generalize these results for larger scales of practical interest and for a range of cover properties and climatological conditions.

Acknowledgments

Financial support by the Swiss National Science Foundation (200021-172493) is gratefully acknowledged. The authors are grateful for access to the FLUXNET data sets. We thank Martin Schmid (EAWAG) for constructive discussions, and greatly appreciate the technical assistance of Hans Wunderli, Daniel Breitenstein, Martina Sommer, and Hannah Wey in laboratory experiments presented in Appendix A and insightful inputs of Ali Ebrahimi in modeling aspects.

Appendix A: Laboratory experiments of evaporation suppression using floating discs

The evaporation suppression from a small water reservoir covered with floating discs was studied experimentally at laboratory scale (Figure A1). To support the modeling assumptions formulated in the

main text, we present here some experimental results (complete results will be published in a separate paper). A square-shaped water reservoir of 1.44 m^2 area and depth 0.16 m was covered with Styrofoam discs of 0.2 m diameter and 0.02 m thickness. The black or white colored discs covered 91% of the water surface. Wind velocities controlled with a wind tunnel and radiation by four light sources were used to create different evaporative forcing. Evaporation suppression was determined by measuring the mass of the water reservoir. Water temperature profile within the reservoir was measured with eight thermocouples. Air temperature, relative humidity and wind velocity were also monitored above the covers. An infrared camera (FLIR SC6000, USA) recorded the surface temperature of the covered reservoir with a spatial resolution of 0.8 mm.

In series of experiments a certain forcing (wind without radiation, radiation with wind and radiation without wind) was maintained for two full days to converge to steady state conditions. The same experimental series were conducted for reservoir without cover and for black and white floating discs. With increasing forcing the evaporation rate for the uncovered reservoir increased from 8 mm/day (radiation without wind) to 14 mm/day (radiation with wind). Independent of the forcing and color of the discs the evaporation rate of the covered reservoir was 20% of the uncovered surface. An evaporation suppression of 80% is less than the cover fraction of 91% that is attributed partially to the increased surface temperature of the water between the discs compared to uncovered water reservoir as shown in Figure A2 and obtained in the modeling results presented in Figure 6.

Hydrol. Earth Syst. Sci. Discuss., https://doi.org/10.5194/hess-2017-415
Manuscript under review for journal Hydrol. Earth Syst. Sci.
Discussion started: 19 July 2017

Hydrology and Earth System Sciences
Discussions

Appendix B: Effective boundary layer thickness over covered reservoirs

We use the analysis of Haghighi and Or (2015b) based on the theory of drag partitioning over rough surfaces (Shao and Yang, 2008; Nepf, 2012) to obtain the effective thickness of viscous sublayer over the covered reservoir:

$$\delta_e = g(\alpha)\frac{\nu}{u_a^*} \tag{B1}$$

where $g(\alpha)$ describes the effect of eddy characteristics (=21 for a practical range), ν is the kinematic viscosity of air, and u_a^* is the air flow friction velocity:

$$u_a^* = U\sqrt{f_r\lambda(1-f_c)C_{rg} + \left(f_s(1-f_c) + f_g f_c\right)C_{sg}} \tag{B2}$$

where U is air flow velocity, and λ is the frontal area index that is a function of disc diameter (d) and height (H):

$$\lambda = N\,d\,H \tag{B3}$$

with N as the number of discs per unit area; $C_{rg} = \gamma C_{sg}$ and C_{sg} are drag coefficients of discs and uncovered surface, respectively with λ=0:

$$C_{sg} = \left(k / \ln\left(z_U / z_{0s}\right)\right)^2 \tag{B4}$$

where z_U and z_{0s} are reference height for measurement of wind velocity and roughness length of uncovered surface, respectively. The parameters f_r, f_s, and f_g are defined as:

Hydrol. Earth Syst. Sci. Discuss., https://doi.org/10.5194/hess-2017-415
Manuscript under review for journal Hydrol. Earth Syst. Sci.
Discussion started: 19 July 2017

$$f_r = \exp\left(-\frac{a_r \lambda}{(1-f_c)^m}\right) \quad \text{(B5)}$$

$$f_s = \exp\left(-\frac{a_s \lambda}{(1-f_c)^m}\right) \quad \text{(B6)}$$

$$f_g = 1+\left(\frac{C_{sgc}}{C_{sg}}-1\right) f_c \quad \text{(B7)}$$

with a_s=5, a_r=3, and m=0.1. The drag coefficient on the surface of disc C_{sgc} is expressed as:

$$C_{sgc} = \left(k / \ln\left(\frac{z_U - H}{z_{0s}}\right)\right)^2 \quad \text{(B8)}$$

By increasing λ from zero (uncovered surface) to $\lambda \approx 0.2$, the interaction of overlying air flow with floating elements results in formation of smaller scale eddies which then decrease the effective thickness of viscous sublayer. Increasing λ more than 0.2 reduces air flow penetration into the gaps which thus traps air between floating elements and forms relatively thick boundary layer in the order of element's height. Figure B1 depicts the effect of cover geometry (diameter and height) on the effective thickness of boundary layer.

Appendix C: The effect of reservoir depth on energy balance

We investigated the effect of reservoir depth on the energy balance and surface heat fluxes considering shallow (3 m) and deep (10 m) hypothetical reservoirs for the conditions in Majadas, Spain (March 2004 to March 2005). The bottom boundary condition was assumed to follow a linear heat flux to the

underlining soil (Shahraeeni and Or, 2011). Although (as expected) the specific energy storage (storage per volume of reservoir) was higher in the shallow reservoir, the surface temperature and heat fluxes were similar for the shallow and deep reservoirs (Table C1). Considering similar aerodynamic conditions at the surface, the similarity in surface fluxes of shallow and deep reservoirs indicate that surface temperatures were similar (e.g., uncovered water surface temperature depicted in Figure C1). These results highlight the dominance of atmospheric forcing in adjusting surface temperature and thus surface heat fluxes whereas the effect of reservoir depth is reflected in the specific energy storage and heat flux at the bottom (especially in uncovered reservoirs), *G*, which is governed by the bottom temperature of the reservoir (Figure C1).

References

Aminzadeh, M., and D. Or (2013), Temperature dynamics during nonisothermal evaporation from drying porous surfaces, Water Resour. Res., 49, 7339–7349, doi:10.1002/2013WR014384.

Aminzadeh, M., and D. Or (2014), Energy partitioning dynamics of drying terrestrial surfaces, J. Hydrol., 519, 1257–1270.

Aminzadeh, M., and D. Or (2017), Pore-scale study of thermal fields during evaporation from drying porous surfaces, Int. J. Heat Mass Transf., 104, 1189-1201, http://dx.doi.org/10.1016/j.ijheatmasstransfer.2016.09.039.

Assouline, S., K. Narkis, and D. Or (2010), Evaporation from partially covered water surfaces, Water Resour. Res., 46, 1–12, doi:10.1029/2010WR009121.

Assouline, S., K. Narkis, and D. Or (2011), Evaporation suppression from water reservoirs: Efficiency considerations of partial covers, Water Resour. Res., 47, 1–8, doi:10.1029/2010WR009889.

Assouline, S., D. Russo, A. Silber, and D. Or (2015), Balancing water scarcity and quality for sustainable irrigated agriculture, Water Resour. Res., 51, 3419–3436, doi:10.1002/2015WR017071.

Chaudhari, N., and N.D. Chaudhari (2015), Use of thermocol sheet as floating cover to reduce evaporation loss in farm pond, in: 20th International Conference on Hydraulics, Water Resources and River Engineering, IIT Roorkee, India.

Cooley, K.R. (1970), Energy relationships in the design of floating covers for evaporation reduction, Water Resour. Res., 6, 717–727, doi:10.1029/WR006i003p00717.

Cooley, K. R. (1983), Evaporation reduction: Summary of long-term tank studies, J. Irrig. Drain. Div. ASCE, 109, 89–98.

Craig, I.P. (2005), Loss of storage water due to evaporation – a literature review, Reports - Univ. South. Queensl., 75.

Dake, J.M.K., and D.R.F. Harleman (1969), Thermal stratification in lakes: Analytical and laboratory studies, Water Resour. Res., 5(2), 484-495.

Dai, A. (2011), Drought under global warming: a review, WIREs Clim. Change, 2: 45–65, doi:10.1002/wcc.81

Foken, T. (2008), The energy balance closure problem: An overview, Ecol. Appl., 18(6), 1351–1367,

doi:10.1890/06-0922.1.

Gaikovich, K.P. (2000), Study of atmospheric-turbulence effects on the formation of a thermal film in the near-surface water layer and the dynamics of air-water heat exchange using measurements of thermal radio emission, Radiophys. Quant. Electron., 43 (6), 469–477, http://dx.doi.org/10.1007/BF02677174.

Gallego-Elvira, B., A. Baille, B. Martin-Gorriz, J.F. Maestre-Valero, and V. Martinez-Alvarez (2011), Energy balance and evaporation loss of an irrigation reservoir equipped with a suspended cover in a semiarid climate (south-eastern Spain), Hydrol. Process., 25, 1694–1703, doi:10.1002/hyp.7929.

Gallego-Elvira, B., A. Baille, B. Martin-Gorriz, J.F. Maestre-Valero, and V. Martinez-Alvarez (2012), Evaluation of evaporation estimation methods for a covered reservoir in a semi-arid climate (south-eastern Spain), J. Hydrol., 458-459, 59–67, doi:10.1016/j.jhydrol.2012.06.035.

Gilau, A.M., and M.J. Small (2008), Designing cost-effective seawater reverse osmosis system under optimal energy options, Renewable Energy, 33, 617-630.

Google Earth 7.1.8.3036 (2017), Hanston, Kansas, US, 38°11’33” N, 99°39’07” W, elevation 660 m; Shahrood, Iran, 36°29’26” N, 54°43’46” W, elevation 1924 m [Available at http://www.google.com/earth/ index.html, Viewed 1 July 2017.].

Gugliotti, M., M.S. Baptista, and M.J. Politi (2005), Reduction of evaporation of natural water samples by monomolecular films, J. Braz. Chem. Soc., 16, 1186–1190, doi:10.1590/S0103-50532005000700015.

Guler, E., G. Onkal Engin, M. Celen, and H. Sari Erkan (2015), Cost analysis of seawater desalination using an integrated reverse osmosis system on a cruise ship, Global NEST J., 17(2), 389-396.

Haghighi, E., E. Shahraeeni, P. Lehmann, and D. Or (2013), Evaporation rates across a convective air boundary layer are dominated by diffusion, Water Resour. Res., 49, 1602–1610, doi:10.1002/wrcr.20166.

Haghighi, E., and D. Or (2013), Evaporation from porous surfaces into turbulent airflows: Coupling eddy characteristics with pore scale vapor diffusion, Water Resour. Res., 49, 8432–8442, doi:10.1002/2012WR013324.

Haghighi, E., and D. Or (2015a), Thermal signatures of turbulent airflows interacting with evaporating thin porous surfaces, Int. J. Heat Mass Transf., http://dx.doi.org/10.1016/j.ijheatmasstransfer.2015.04.026.

Haghighi, E., and D. Or (2015b), Interactions of bluff-body obstacles with turbulent airflows affecting evaporative fluxes from porous surfaces, J. Hydrol., 530, 103-116.

Henderson-Sellers, B. (1985), New formulation of eddy diffusion thermocline models, Appl. Math. Modelling, 9, 441-446.

Kalma, J. D., T. R. McVicar, and M. F. McCabe (2008), Estimating land surface evaporation: A review of methods using remotely sensed surface temperature data, Surv. Geophys., 29, 421–469, doi:10.1007/s10712-008-9037-z.

Lehner, B., C. R. Liermann, C. Revenga, C. Vörösmarty, B. Fekete, P. Crouzet, P. Döll, M. Endejan, K.

Frenken, J. Magome, C. Nilsson, J. Robertson, R. Rödel, N. Sindorf, and D. Wisser (2011), High resolution mapping of the world's reservoirs and dams for sustainable river flow management, Frontiers in Ecology and the Environment.

Malacic, V. (1991), Estimation of the vertical eddy diffusion coefficient of heat in the Gulf of Trieste (Northern Adriatic), Oceanol. Acta, 14(1), 23–32.

McCormick, M.J., and D. Scavia (1981), Calculation of vertical profiles of lake-averaged temperature and diffusivity in Lakes Ontario and Washington, Water Resour. Res., 17(2), 305–310.

Moreo, M.T., and A. Swancar (2013), Evaporation from Lake Mead, Nevada and Arizona, March 2010 through February 2012: U.S. Geological Survey Scientific Investigations Report 2013–5229, 40 p., http://dx.doi.org/10.3133/sir20135229.

Nepf, H.M. (2012), Hydrodynamics of vegetated channels, J. Hydraul. Res., 50 (3), 262–279, http://dx.doi.org/10.1080/00221686.2012.696559.

Priestley, C., and R. Taylor (1972), On the assessment of surface heat flux and evaporation using large-scale parameters, Mon. Weather Rev., 81–92.

Rabl, A., and C.E. Nielsen (1975), Solar ponds for space heating, Solar Energy, 17, 1–12.

Ruskowitz, J.A., F. Suarez, S.W. Tyler, and A.E. Childress (2014), Evaporation suppression and solar energy collection in a salt-gradient solar pond, Sol. Energy., 99, 36–46, doi:10.1016/j.solener.2013.10.035.

Rost, S., D. Gerten, A. Bondeau, W. Luncht, J. Rohwer, and S.Schaphoff (2008), Agricultural green and blue water consumption and its influence on the global water system, Water Resour. Res., 44, W09405, doi:10.1029/2007WR006331.

Schladow, S.G., M. Lee, B.E. Hürzeler, and P.B. Kelly (2002), Oxygen transfer across the air-water interface by natural convection in lakes, Limnol. Oceanogr., 47, 1394–1404.

Schlünder, E.U. (1988), On the mechanism of the constant drying rate, Chem. Eng. Sci., 43, 2685–2688.

Shahraeeni, E., and D. Or (2011), Quantification of subsurface thermal regimes beneath evaporating porous surfaces, Int. J. Heat Mass Transf., 54, 4193–4202, doi:10.1016/j.ijheatmasstransfer.2011.05.024.

Shahraeeni, E., P. Lehmann, and D. Or (2012), Coupling of evaporative fluxes from drying porous surfaces with air boundary layer: Characteristics of evaporation from discrete pores, Water Resour. Res., 48, 1–15, doi:10.1029/2012WR011857.

Shao, Y., and Y. Yang (2008), A theory for drag partition over rough surfaces, J. Geophys. Res., 113, F02S05, http://dx.doi.org/10.1029/2007JF000791.

Shilo, E., B. Ziv, E. Shamir, and A. Rimmer (2015), Evaporation from lake Kinneret, Israel, during hot summer days, J. Hydrol., 528, 264–275.

Stefan, H.G., X. Fang, D. Wright, J.G. Eaton, and H. Mccormick (1995), Simulation of dissolved oxygen profiles in a transparent, dimictic lake, Limnol. Oceanogr. , 40, 105–118.

Vercauteren, N., H. Huwald, E. Bou-Zeid, J.S. Selker, U. Lemmin, M.B. Parlange, and I. Lunati (2011), Evolution of superficial lake water temperature profile under diurnal radiative forcing, Water Resour. Res., 47, 1–10. doi:10.1029/2011WR010529.

Vlasov, M. N., and M. C. Kelley (2014), Criterion for analyzing experimental data on eddy diffusion coefficients, Ann. Geophys., 32(6), 581–588, doi:10.5194/angeo-32-581-2014.

Wilkinson, G.M., J.J. Cole, M.L. Pace, R.A. Johnson, and M.J. Kleinhans (2015), Physical and biological contributions to metalimnetic oxygen maxima in lakes, Limnol. Oceanogr., 60, 242–251, http://dx.doi.org/10.1002/lno.10022.

Yao, X., H. Zhang, C. Lemckert, and A. Brook (2010), Evaporation reduction by suspended and floating covers: Overview, modelling and efficiency, Urban Water Security Research Alliance Technical Report, 28.

Hydrol. Earth Syst. Sci. Discuss., https://doi.org/10.5194/hess-2017-415
Manuscript under review for journal Hydrol. Earth Syst. Sci.
Discussion started: 19 July 2017

Hydrology and Earth System Sciences Discussions

Table 1: The physical properties of water and the Styrofoam discs (white and black surfaces) used for modeling.

	Specific heat (J/kg K)	Emissivity	Albedo	Thermal conductivity (W/mK)	Molecular thermal diffusivity (m^2/s)
Water	4200	0.95	0.05	0.6	1.43×10^{-7}
Discs	1131	0.85	white: 0.6 black: 0.1	0.03	3.9×10^{-8}

Table 2: Comparison of model estimates for uncovered water surface with measurements of annual surface energy balance components for Lake Mead (2010-2011).

	Rn (W/m^2)	LE (W/m^2)	E (mm/day)	H (W/m^2)
Measurements (Bowen ratio EB)	147	170	5.95	-18
Model estimates	187	148	5.2	-36

Table 3: Modeled annual surface heat fluxes of uncovered and covered hypothetical reservoir in Majadas, Spain (March 2004 to March 2005).

	Rn (W/m^2)	LE (W/m^2)	E (mm/day)	E (mm/year)	H (W/m^2)
Uncovered	147.9	127.3	4.48	1635	-65.1
Covered with black discs	122.1	14.5	0.51	187	94.9
Covered with white discs	54.8	12.9	0.45	167	30.7

Hydrol. Earth Syst. Sci. Discuss., https://doi.org/10.5194/hess-2017-415
Manuscript under review for journal Hydrol. Earth Syst. Sci.
Discussion started: 19 July 2017

Hydrology and Earth System Sciences
Open Access
Discussions

Table C1: The effect of reservoir depth on heat fluxes and specific storage of uncovered and covered reservoirs.

		Rn (W/m^2)	H (W/m^2)	G (W/m^2)	E (mm/day)	Storage: June-Sep (MJ/m^3)
3 m depth	Uncovered	148.7	-67	29.2	4.43	**25**
	Covered with black discs	122.9	92.7	2.2	0.44	2.1
	Covered with white discs	55.4	28.5	1.8	0.39	1.6
10 m depth	Uncovered	148.1	-65.6	20.4	4.46	**18.4**
	Covered with black discs	122.5	93.8	2.2	0.47	1.9
	Covered with white discs	55.1	29.5	2.1	0.41	1.3

Hydrol. Earth Syst. Sci. Discuss., https://doi.org/10.5194/hess-2017-415
Manuscript under review for journal Hydrol. Earth Syst. Sci.
Discussion started: 19 July 2017

Hydrology and Earth System Sciences
Open Access
Discussions

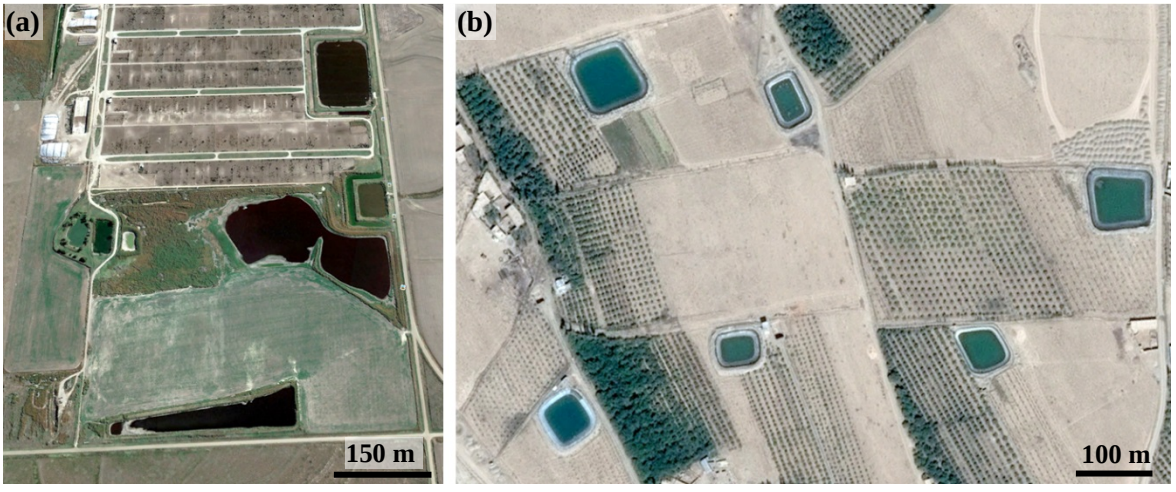

Figure 1: The growing number of small reservoirs for local supply during dry periods highlights the need for evaporation suppression measures to conserve water (satellite images from (a) Hanston, Kansas, US, and (b) Shahrood, Iran; reproduced from Google Earth (2017)).

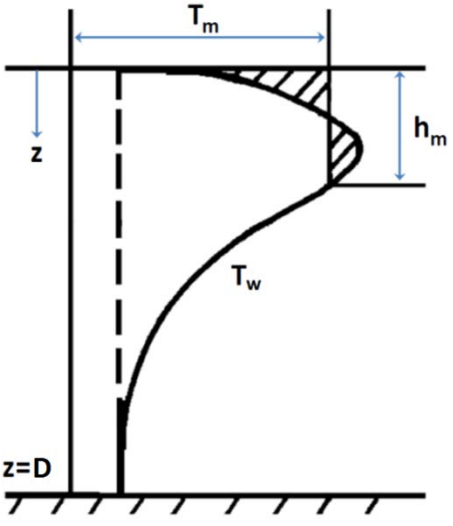

Figure 2: Convective mixing at the surface of water reservoir of depth *D* due to the unstable temperature profile associated with subsurface radiation absorption (adapted from Dake and Harleman (1969)). Based on Eq. (10), the hatched areas on the left and right hand side of T_m are equal representing transfer of subsurface heat accumulation to the surface.

Hydrol. Earth Syst. Sci. Discuss., https://doi.org/10.5194/hess-2017-415
Manuscript under review for journal Hydrol. Earth Syst. Sci.
Discussion started: 19 July 2017

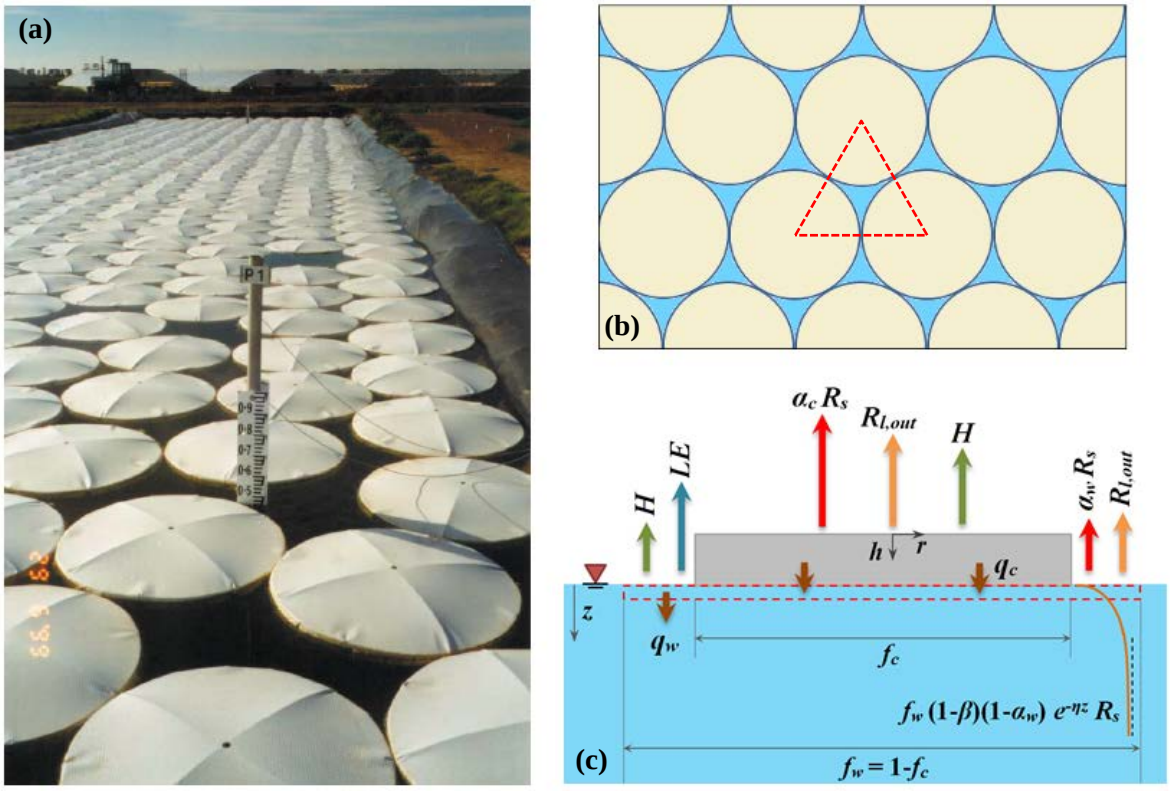

Figure 3: (a) Application of floating discs in suppressing evaporative loss from water reservoirs (adapted from Assouline et al. (2011)); (b) top view of reservoir surface covered with discs; due the geometrical constraints, dense packing of discs provides a surface coverage of 0.91 (inferred from the depicted triangle with side lengths equal to disc diameter); (c) schematic representation of subsurface radiation attenuation and surface heat fluxes in a representative unit cell including a floating element and free water surrounding it with areal fractions of f_c and f_w, respectively (see Eq. 12).

Hydrol. Earth Syst. Sci. Discuss., https://doi.org/10.5194/hess-2017-415
Manuscript under review for journal Hydrol. Earth Syst. Sci.
Discussion started: 19 July 2017

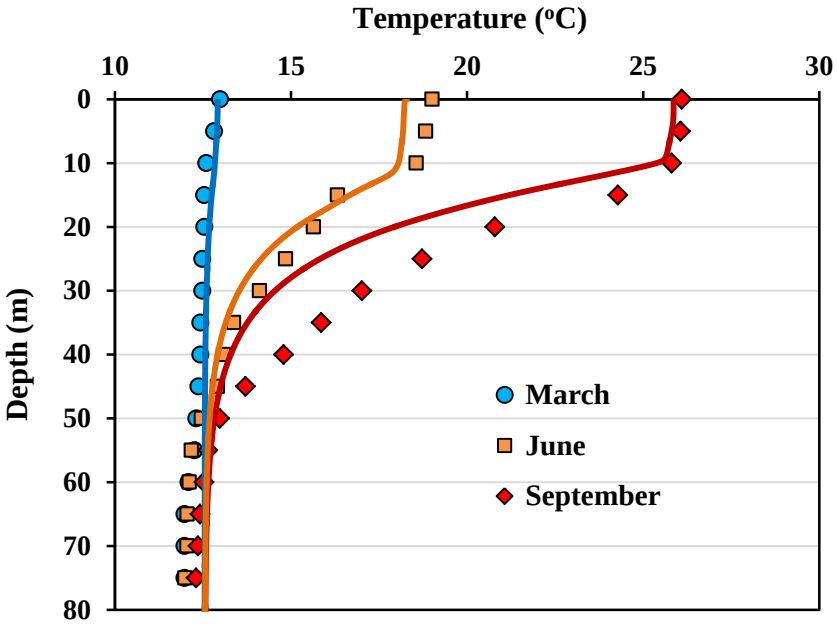

Figure 4: Model predictions (lines) and measurements (symbols) (Moreo and Swancar, 2013) of mean monthly vertical temperature profiles in Lake Mead; modeling results were obtained using meteorological data measured at Lake Mead assuming radiation absorption at surface (β) and attenuation coefficient (η) of 0.3 and 0.1, respectively.

Hydrol. Earth Syst. Sci. Discuss., https://doi.org/10.5194/hess-2017-415
Manuscript under review for journal Hydrol. Earth Syst. Sci.
Discussion started: 19 July 2017

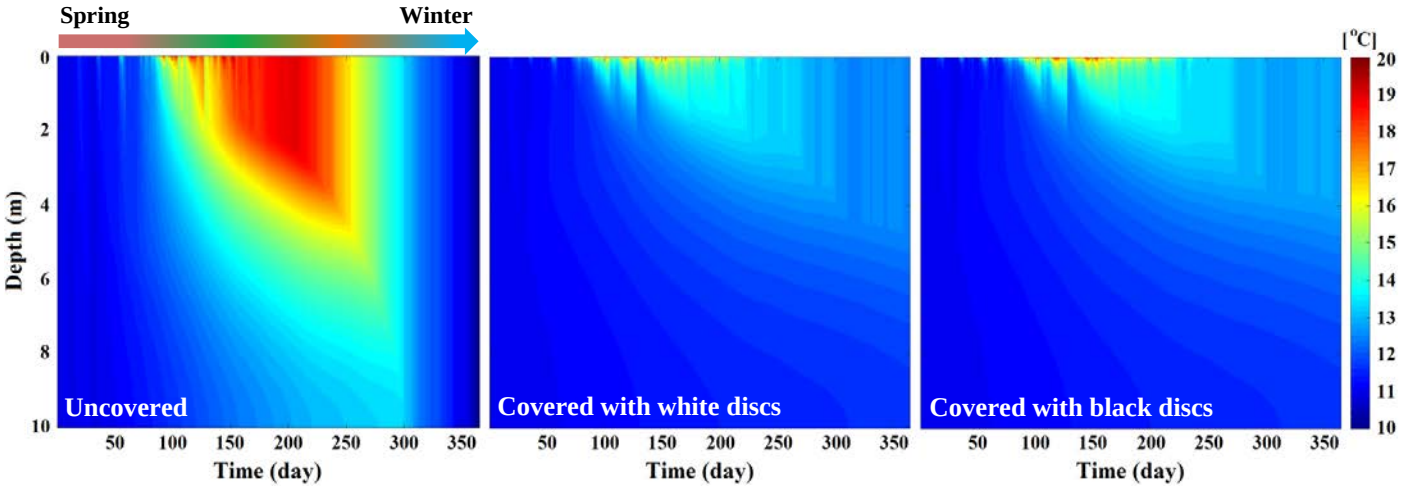

Figure 5: Modeling the effect of surface coverage on mean daily temperature in a hypothetical reservoir with 10 m depth using meteorological data from FLUXNET in Majadas, Spain (March 2004 to March 2005); the reservoir was covered using white and black Styrofoam discs (diameter: 0.2 m and height: 0.02 m) that provide 0.91 coverage of the reservoir surface. A uniform vertical temperature at 11 °C was assumed as the initial condition, and the bottom boundary condition was set to zero heat flux.

Hydrol. Earth Syst. Sci. Discuss., https://doi.org/10.5194/hess-2017-415
Manuscript under review for journal Hydrol. Earth Syst. Sci.
Discussion started: 19 July 2017

Hydrology and Earth System Sciences
Discussions

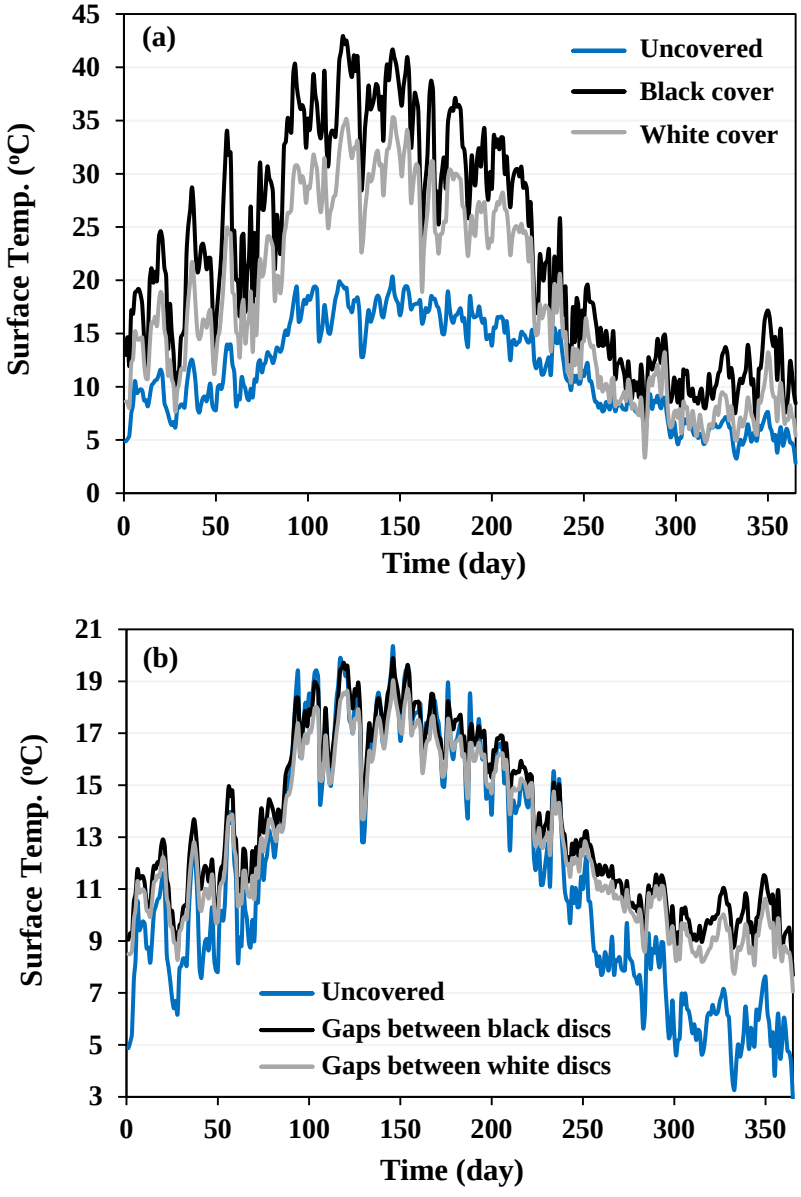

Figure 6: (a) The evolution of temperature on the top surface of floating discs and on the surface of uncovered reservoir; (b) comparing surface temperature of the uncovered water reservoir with temperature at the surface of water gaps between floating elements.

Hydrol. Earth Syst. Sci. Discuss., https://doi.org/10.5194/hess-2017-415
Manuscript under review for journal Hydrol. Earth Syst. Sci.
Discussion started: 19 July 2017

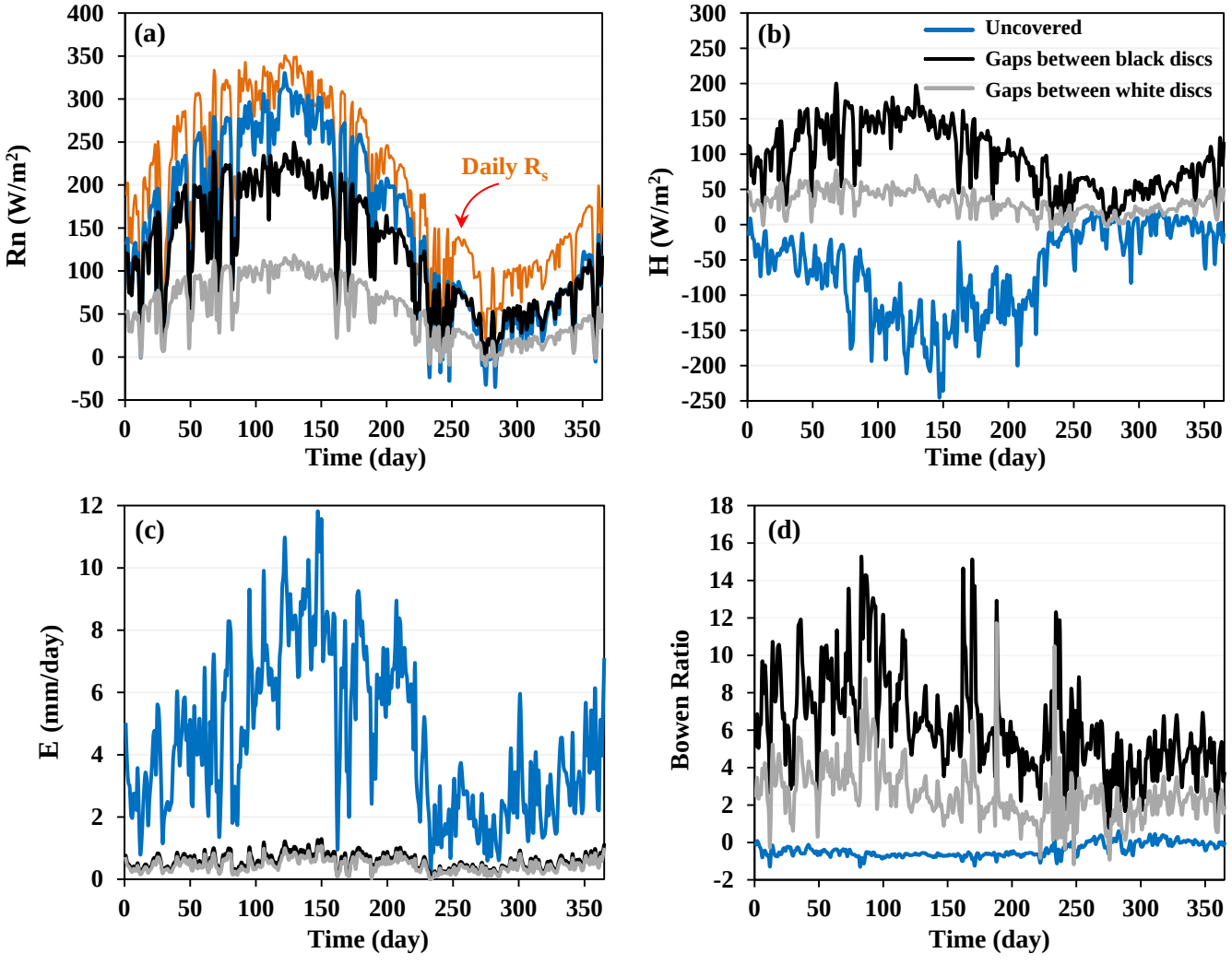

Figure 7: Model estimates for the evolution of net radiation (a), sensible heat flux (b), evaporation rate (c), and Bowen ratio (d) for uncovered and partially covered reservoir with black and white Styrofoam discs for the FLUXNET data from Majadas, Spain (March 2004 to March 2005). Mean daily incoming solar radiation is marked in (a).

Hydrol. Earth Syst. Sci. Discuss., https://doi.org/10.5194/hess-2017-415
Manuscript under review for journal Hydrol. Earth Syst. Sci.
Discussion started: 19 July 2017

Hydrology and Earth System Sciences
Discussions

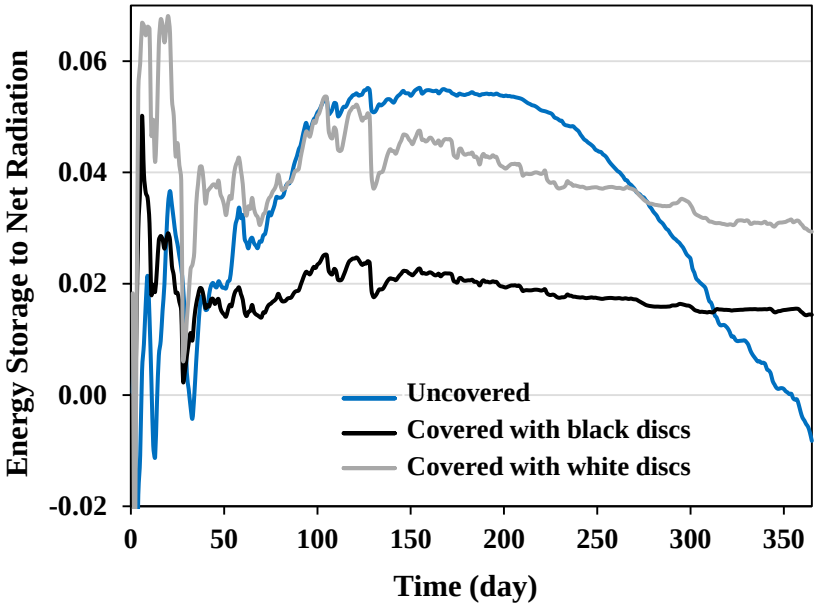

Figure 8: Model estimates of changes in the ratio of energy storage in the water body to the net radiative flux at the surface of uncovered and partially covered hypothetical 10 m deep reservoir (Majadas, Spain).

Hydrol. Earth Syst. Sci. Discuss., https://doi.org/10.5194/hess-2017-415
Manuscript under review for journal Hydrol. Earth Syst. Sci.
Discussion started: 19 July 2017

Hydrology and Earth System Sciences
Discussions

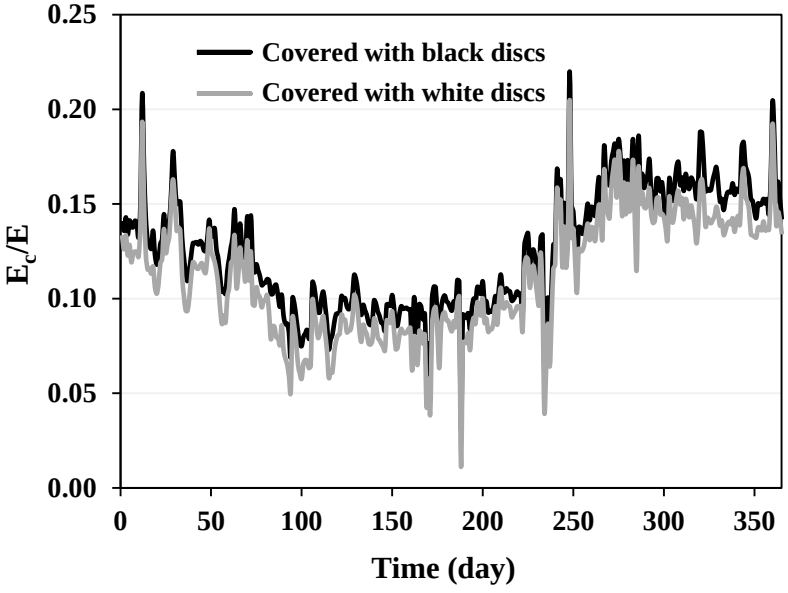

Figure 9: The ratio of evaporation from covered (E_c) to uncovered water reservoir (E) representing evaporation suppression efficiency of floating elements (for the meteorological conditions in Majadas, Spain from March 2004 to March 2005).

Hydrol. Earth Syst. Sci. Discuss., https://doi.org/10.5194/hess-2017-415
Manuscript under review for journal Hydrol. Earth Syst. Sci.
Discussion started: 19 July 2017

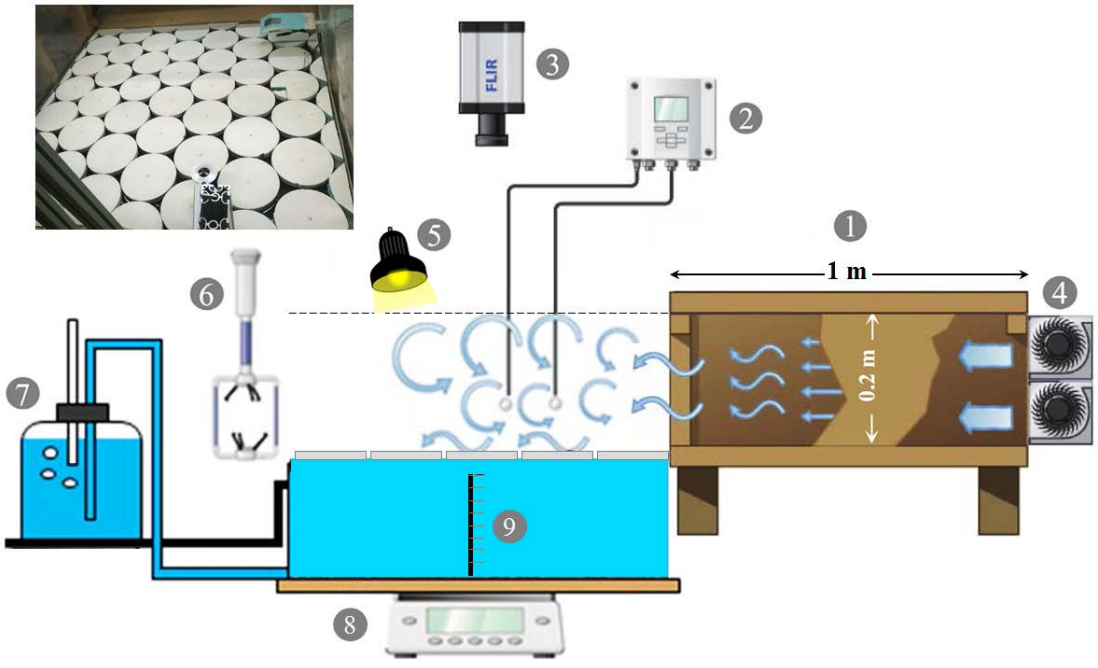

Figure A1: Experimental setup for evaporation suppression measurements from a small water basin covered with floating discs: (1) wind tunnel, (2) air temperature and humidity sensors (Vaisala HUMICAP, HMT337, Finland), (3) IR camera (FLIR SC6000, USA), (4) tunable fans generating wind flow, (5) xenon lamps for shortwave radiation, (6) high-frequency 3D sonic anemometer (WindMaster, Gill Instruments Ltd., The Netherlands), (7) Mariotte bottle to adjust water level, (8) balance to determine mass loss and evaporation rates, (9) temperature sensors in water body.

Hydrol. Earth Syst. Sci. Discuss., https://doi.org/10.5194/hess-2017-415
Manuscript under review for journal Hydrol. Earth Syst. Sci.
Discussion started: 19 July 2017

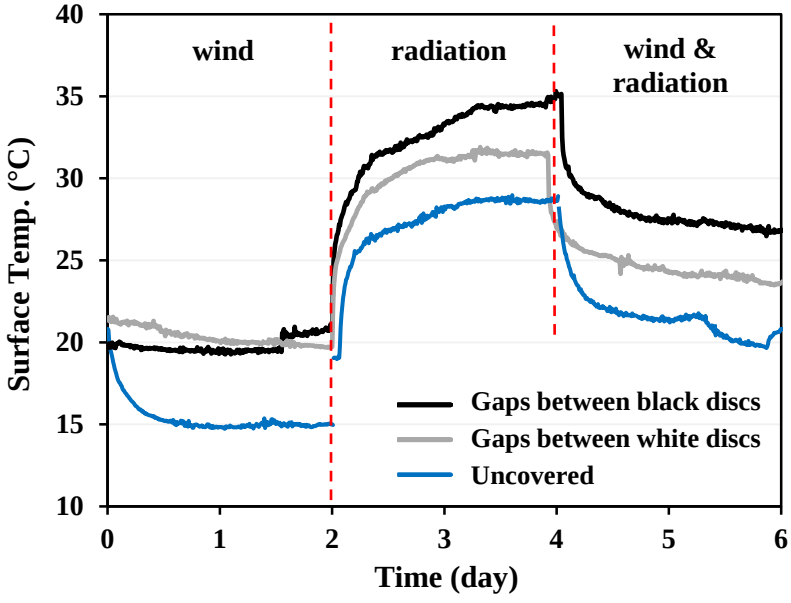

Figure A2: Surface temperature of uncovered water reservoir and gaps between white and black discs obtained from IR measurements.

Hydrol. Earth Syst. Sci. Discuss., https://doi.org/10.5194/hess-2017-415
Manuscript under review for journal Hydrol. Earth Syst. Sci.
Discussion started: 19 July 2017

Hydrology and Earth System Sciences
Discussions

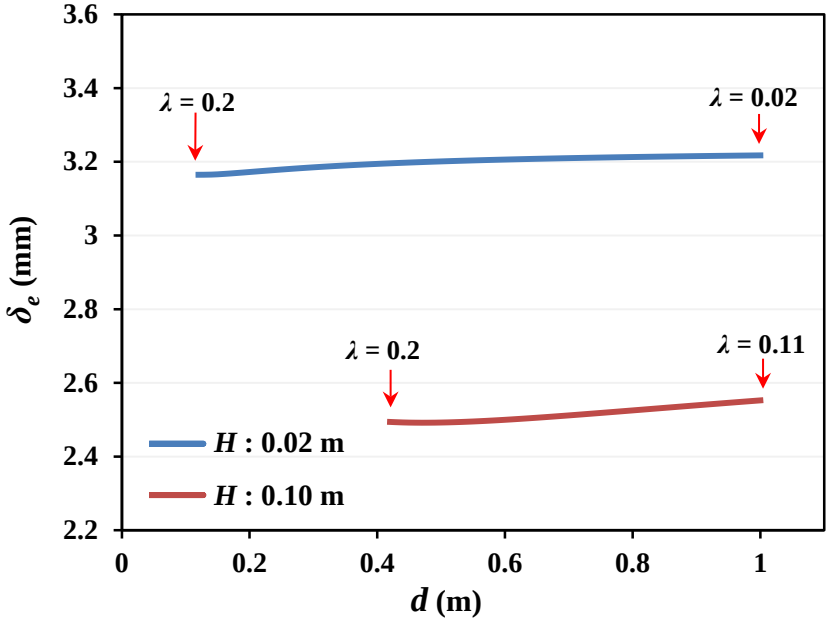

Figure B1: Variation of effective boundary layer thickness with disc diameter (*d*) for different disc heights (*H*) at wind speed of 1 m/s and surface coverage of 0.91 (dense packing). The increase of λ more than 0.2 forms relatively thick boundary layer in the order of disc height. For *U*=1 m/s, the boundary layer thickness over uncovered surface is calculated as 3.2 mm based on Haghighi and Or (2013).

Hydrol. Earth Syst. Sci. Discuss., https://doi.org/10.5194/hess-2017-415
Manuscript under review for journal Hydrol. Earth Syst. Sci.
Discussion started: 19 July 2017

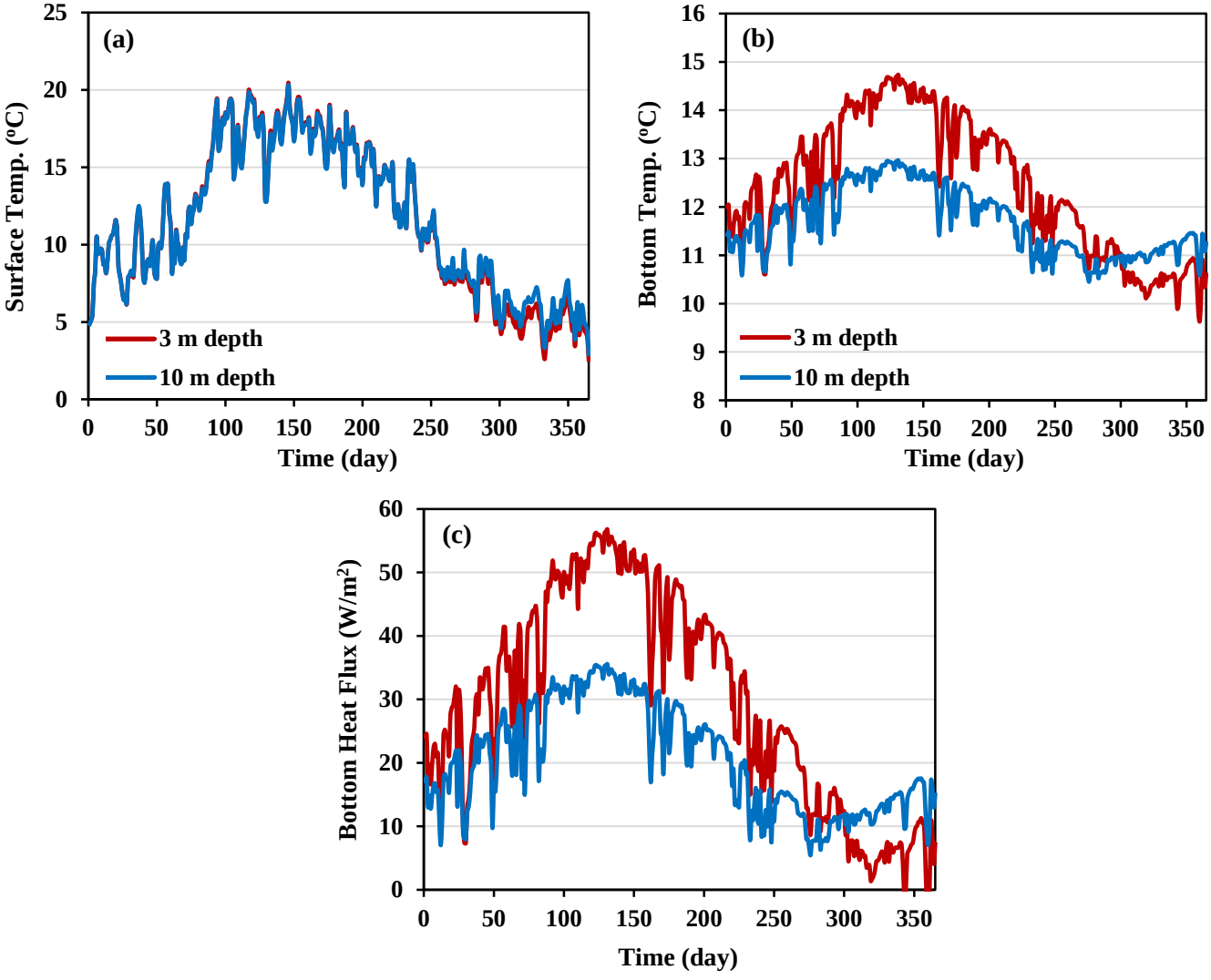

Figure C1: The effect of reservoir depth on surface (a) and bottom (b) temperature of the uncovered reservoir considering bottom heat flux towards the underlining soil layer (c); T_{sZ} was assumed at 10 °C.